

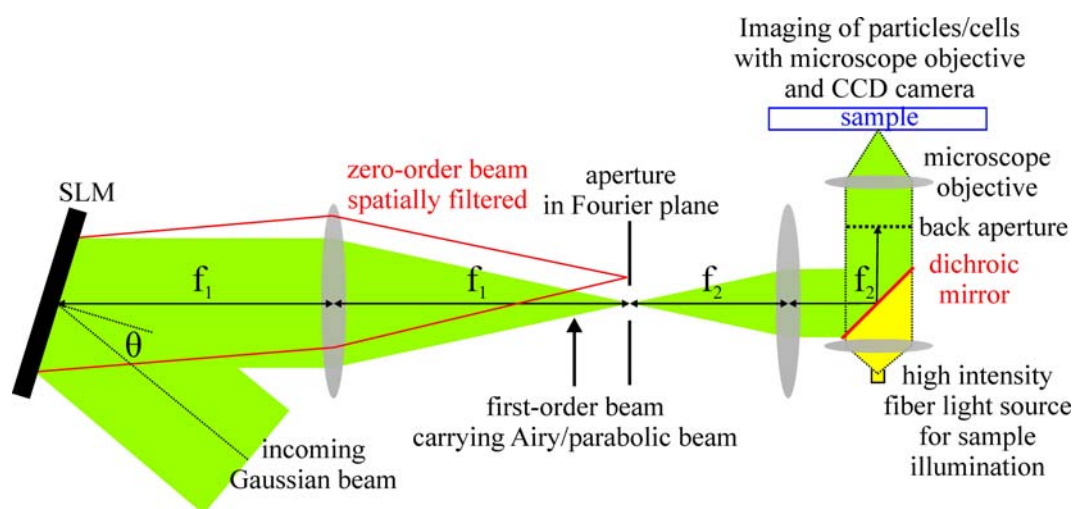
## Optical redistribution of microparticles and cells between microwells

Jörg Baumgartl,<sup>a</sup> Gregor M. Hannappel,<sup>a</sup> David J. Stevenson,<sup>a</sup>  
Daniel Day,<sup>b</sup> Min Gu<sup>b</sup> and Kishan Dholakia<sup>a</sup>

<sup>a</sup>*SUPA, School of Physics and Astronomy, University of St. Andrews, St. Andrews, Fife, KY16 9SS, UK. E-mail: jb211@st-andrews.ac.uk*

<sup>b</sup>*Centre for Micro-Photonics, Faculty of Engineering and Industrial Sciences, Swinburne University of Technology, Hawthorn, 3122, Victoria, Melbourne, Australia*

### Experimental setup



**Supplementary Fig. 1** Experimental setup: the black rectangle indicates the spatial light modulator (SLM). Grey ellipses represent lenses (focal widths  $f_1 = 1$  m and  $f_2 = 315$  mm), the microscope objective (magnification 40x, NA = 0.65) and the lens to collimate the light source for sample illumination.  $\theta$  denotes the angle of incidence. The sketch is a simplified two-dimensional illustration of the setup; in a full three-dimensional illustration, the optical path through the sample plane would be perpendicular to the drawing plane. See text for a detailed description.

Our experiments were performed using a linearly polarized Ar<sup>+</sup> laser ( $\lambda = 514$  nm,  $P_{\max} = 7$  W). The output power was  $P = 1.5$  W, and the beam intensities were then adjusted using a half wave plate and a polarising beam splitter. A beam expander both increased the beam diameter and collimated the beam which was then incident onto the chip of a spatial light modulator (SLM, Hamamatsu LCOS X10468-04, chip dimensions: 16 mm x 12 mm, 800 pixel x 600 pixel, diffraction efficiency  $\approx 90\%$ ). The beam slightly overfilled the chip and the angle of incidence  $\theta$  was  $1.5^\circ$  (see Supplementary Fig. 1). Following the approach presented in ref. 1, the SLM was used to impose a cubic phase modulation onto the incident Gaussian beam using the central, 600 pixel x 600 pixel area of the SLM chip. The modulated beam was subsequently Fourier-transformed into the Airy beam (see next paragraph for the creation of parabolic beams) using a spherical lens (focal width  $f_1 = 1$  m) which had a distance of  $f_1 = 1$  m from the SLM as illustrated in Supplementary Fig. 1. Imposing an additional linear phase modulation onto the incident beam allowed us to relocate the Airy beam in the Fourier plane at will (as described in more detail below) and, in particular, to separate the Airy beam from the zero-order reflection of the SLM which is spatially filtered using an aperture. Finally, the Airy beam was downsized by an inverse telescope (size of the beam's main spot  $\approx 3$   $\mu\text{m}$ ) and imaged from below into a sample chamber which is described further

below. The inverse telescope consisted of a spherical lens (focal width  $f_2 = 315$  mm) and a microscope objective (magnification 40x, NA = 0.65). The distance between the spherical lens and the back aperture of the objective matched the focal width  $f_2$ . Using this particular configuration the Airy beam was always fully transmitted through the back aperture of the objective irrespective of the beam position in the Fourier plane. Overall, our setup allowed us to create a relocatable Airy beam featuring a transverse parabolic deflection of 10  $\mu\text{m}$  after a propagation distance of 60  $\mu\text{m}$  in the sample chamber (see Fig. 1(a) of our communication). Note that we were able to increase the transverse parabolic deflection up to 15  $\mu\text{m}$  after a propagation distance of 60  $\mu\text{m}$ . This was achieved by slightly increasing the distance between the inverse telescope lenses by a few millimetres (see supplementary information associated with ref. 2).

Parabolic beams were created in a similar manner to Airy beams by imposing a cubic phase modulation onto a Gaussian laser beam. However, an additional one-dimensional amplitude modulation of the Gaussian laser beam was required.<sup>3</sup> The amplitude modulation obeys the eigenfunctions of the quartic oscillator which were calculated recursively.<sup>4</sup> Intuitively, the phase mask displayed on the SLM was reduced to a central part ( $\approx 600$  pixel  $\times$  150 pixel). This central part was cut into  $n+1$  slices ( $n$  integer,  $n > 0$ ) to create parabolic beams of  $n$ -th order where a phase shift of  $\pi$  was imposed on every second slice. As result, the  $n+1$  slice modulation of the phase mask created the  $n+1$  tail structure of parabolic beams of  $n$ -th order as shown in Fig. 1(b)-(d) of our communication. Note that we used the approach put forward in ref. 5 to encode both amplitude and phase information onto a phase-only SLM. This is an approximative approach creating so-called 'ghost beams' at integer multiples of the deflection of the first-order beam. However, these 'ghost beams' were too weak in our experiments to influence the motion of particles/cells in the sample chamber. Finally, note that parabolic beams only carry a small fraction ( $\approx 20\%$ ) of the intensity of Airy beams because of the different phase mask sizes used; a full size phase mask was used for Airy beams, and only a central slice was used for parabolic beams. To aid comparison between these light fields, we reduced the Airy beam intensity by multiplying the corresponding phase mask with a factor  $0 < a < 1$  following the approximative approach described in ref. 5. The effective laser powers in the sample plane were 25 mW.

Particles/Cells were illuminated from below using a high intensity fibre light source (Thorlabs OSL 1-EC) and imaged from above with a long-distance microscope objective (Mitutoyo, magnification 20x, NA = 0.28) onto a CCD camera (Watec WAT-902B), as indicated in Supplementary Fig. 1. Relocation of the microscope objective allowed us to observe the redistribution of particles/cells in different transverse planes along the beam propagation axis. This was important to characterise and verify the redistribution effect presented in our communication. Note, however, that we also managed to implement our setup into a standard inverted optical microscope (Nikon TE2000) using the imaging objective as the second lens of the inverse telescope which downsizes the Airy/parabolic beam. This facilitates the use of coverslip-bottomed Petri dishes, commonly used in cell culture, instead of the custom sample chambers described in the next section.

The Airy/parabolic beams could be relocated in the sample plane across the area covered by four neighbouring microwells ( $\approx 200$   $\mu\text{m}$   $\times$  200  $\mu\text{m}$ ). This was achieved by appropriately changing the linear phase modulation imposed onto the incident Gaussian beam by the SLM (for instance, see ref. 6 for an in-depth explanation). In addition, the orientation of the Airy/parabolic beams in the sample plane could be changed at will through an appropriate rotation of the cubic phase modulation displayed on the SLM. We developed a Labview program which allowed us to both relocate and reorientate the Airy/parabolic beams by simply drawing a line on a recorded image. The line starting point and the line orientation determined the beam position and the beam orientation, respectively. The respective calibration factors, which translate the image scale to the SLM display scale, were easily obtained by drawing lines for two different given beam positions

and orientations.

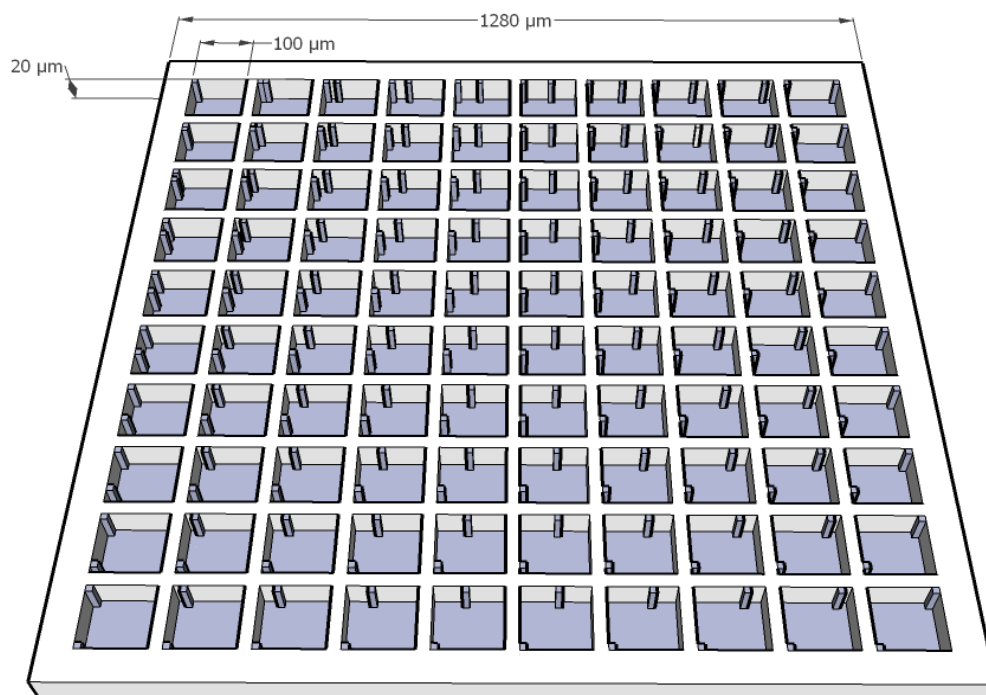
### Sample preparation

In our experiments we used sample chambers which consisted of two cover slips separated by a vinyl spacer (20 mm x 20 mm square, with a central circular cutout of diameter = 10 mm, and a thickness  $\approx 50 \mu\text{m}$ ). We stacked two spacers to achieve sample heights of 100  $\mu\text{m}$ , at least, to avoid the possibility of levitated particles/cells reaching and adhering to the top cover slip. The 10 x 10 array of microwells was created as described below and then put onto the bottom coverslip in the centre of the vinyl spacer opening. Finally, we placed an aqueous suspension of polymer particles (radius  $R=2.85 \mu\text{m}$ , IDC sulfate latex), heparinised human blood, or Chinese Hamster Ovary (CHO) cells that had phagocytosed polymer spheres ( $R=1.5 \mu\text{m}$ ) into the sample chamber prior to sealing the chamber with a cover slip.

Human blood was taken and placed into heparinised containers (Becton-Dickinson Vacutainer tubes type NH 170 IU 10 ml). It was diluted 1:100 into Hanks Balanced Salt Solution (Sigma, UK) and placed onto either glass coverslips or PDMS microwells. CHO K1 cells were routinely kept in a humidified atmosphere of 5%  $\text{CO}_2$  / 95% air at 37 °C in Modified Earles Medium (MEM) with 10% foetal calf serum (FCS) (Globepharm, Surrey, UK), 20 enzyme units/ml of penicillin (Sigma, UK) and 20  $\mu\text{g}/\text{ml}$  of streptomycin (Sigma, UK). Cells that had been exposed to polymer spheres ( $R=1.5 \mu\text{m}$ ) for 24h (Nuncleon, Fisher Scientific, UK) were rendered non-adherent and non-adhesive by suspending in 1 ml trypsin-EDTA (Sigma, UK) throughout the duration of the experiment ( $< 30 \text{ min}$ ). For PDMS microwell pacification to prevent adhesion, a solution of 20 mg/ml poly-2-hydroxyethylmethacrylate (Sigma, UK) in 95% ethanol was added and allowed to evaporate prior to the addition of the cell solution.<sup>7</sup> We have also performed test measurements in samples which did not contain the PDMS microwell structure. In this case, SigmaCote (Sigma, UK) was added and allowed to evaporate for glass surface pacification.

### Manufacturing of microwells

The microwell structures (see Supplementary Fig. 2) were produced by direct laser writing of a negative mold from which the microwells could be replicated.<sup>8</sup> An amplified femtosecond pulse laser (Spitfire, Newport Spectra-Physics, USA) was used to etch a negative mold of the microwells in a poly(methyl methacrylate) (PMMA) substrate. The amplified femtosecond pulse laser directly ionizes the PMMA substrate in the focal spot of the focusing objective lens with no thermal damage to the surrounding material, which enables the etching of micrometer sized structures. The PMMA substrate is mounted on a three-dimensional translation stage that is controlled by a Labview program, which when combined with the selective etching from a femtosecond pulse laser enables the fabrication of three-dimensional structures. After the fabrication the mold was cleaned in an ultrasonic bath for 5 minutes, rinsed with isopropanol, and dried with nitrogen. Poly(dimethyl siloxane) (PDMS) (Sylgard 184, Dow Corning, USA) is used to replicate the microwells. The PDMS was prepared by combining the base and cure components in the ratio of 10:1 in a glass vial. After thoroughly mixing the two components the glass vial was placed under a vacuum for 10 minutes to remove the air bubbles, and the mixed PDMS was then poured over the mold. A second substrate (a glass slide) was then placed on top of the mold and heated on a hotplate at 80 °C for one hour to allow the PDMS to cure to its final state. Once cured, the glass slide with the replicated microwell structures was peeled off the mold. Afterwards, the microwell structure was peeled off the glass slide using metal tweezers and put onto the bottom plate of our sample chamber. The structure comprised 10 x 10 microwells each 100  $\mu\text{m}$  x 100  $\mu\text{m}$  in size. The separating walls had a height of 20  $\mu\text{m}$ .



**Supplementary Fig. 2** The PDMS array of microwells. Note each microwell also contained reference posts to easily find the XY position of a well-of-interest.

## References

- 1 G. A. Siviloglou, J. Broky, A. Dogariu and D. N. Christodoulides, *Phys. Rev. Lett.*, 2007, **99**, 213901.
- 2 J. Baumgartl, M. Mazilu and K. Dholakia, *Nature Photon.*, 2008, **2**, 675.
- 3 J. A. Davis, M. J. Mintry, M. A. Bandres and D. M. Cottrell, *Opt. Express*, 2008, **16**, 12866.
- 4 K. Banerjee *et al.*, *Proceedings of the Royal Society of London. Series A, Mathematical and Physical Sciences*, 1978, **360**, 575.
- 5 J. A. Davis *et al.*, *Appl. Opt.*, 1999, **38**, 5004.
- 6 Spalding *et al.*, in *Structured Light and its Applications: An Introduction to Phase-Structured Beams and Nanoscale Optical Forces*, edited by D. L. Andrews, 2008, p. 139.
- 7 R. J. Clarke, K. Hognason, M. Brimacombe and E. Townes-Anderson, *Mol. Vis.*, 2008, **14**, 706.
- 8 D. Day *et al.*, *Immunol. Cell Bio.*, 2009, **87**, 154.